

# Asymptotic and numerical investigations on viscoelastic fluid flows

Irineu Lopes Palhares Junior

FCT/UNESP,  
[irineu.palhares@unesp.br](mailto:irineu.palhares@unesp.br)



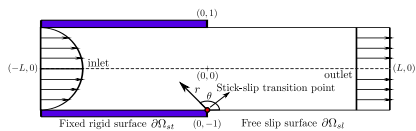
# Summary

- 1 Introduction
- 2 Governing equations
- 3 Asymptotic results
- 4 Numerical results
- 5 Conclusion

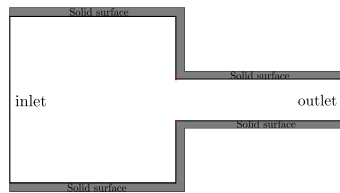


# Introduction

- Flows with singularities are particularly challenging for viscoelastic fluids.
- These may arise due to a non-smooth flow domain or a sudden change in flow conditions.



Stick-slip flow [2]



4:1 contraction flow [4]

Figura 1: Benchmark flows with singularities.

- The treatment of such singularities and associated high stress concentrations is one of the most challenging problems in computational non-Newtonian fluid mechanics.



# Main goals

- This work investigates the stresses of PTT, Giesekus, and Oldroyd-B fluids in a Newtonian velocity field near the stick-slip singularity;
- The stresses of the Oldroyd-B model are defined in a Newtonian velocity field;
- The asymptotic behaviour are verified by integrating the constitutive equations along streamlines and with a full numerical code.



# Problem formulation

The limit of large surface tension yields an undeformable free surface, giving the so-called stick-slip problem.

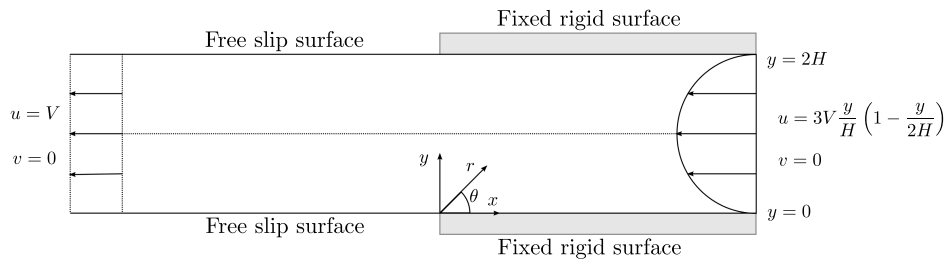


Figura 2: Geometry of the stick-slip problem.



# A three-region asymptotic structure

We expect a three region structure near the singularity composed of a core region with narrow boundary layers at stick and slip surfaces.

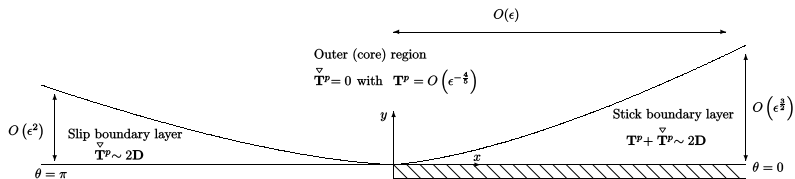


Figura 3: Asymptotic structure local to the singularity for small length scales  $\epsilon$  [1].



# Governing equations

The governing equations for steady, planar, and incompressible creeping flow are taken in the dimensionless form

$$\nabla \cdot \mathbf{v} = 0, \quad 0 = -\nabla p + \nabla \cdot \mathbf{T}, \quad \mathbf{T} = \beta \mathbf{T}^s + (1 - \beta) \mathbf{T}^p, \quad (1)$$

$$\mathbf{T}^s = 2\mathbf{D}, \quad \mathbf{T}^p + Wi \left( \nabla \mathbf{T}^p + \kappa g(\mathbf{T}^p) \right) = 2\mathbf{D}, \quad (2)$$

where

$$g(\mathbf{T}^p) = \begin{cases} 0, & \text{Oldroyd-B,} \\ tr(\mathbf{T}^p) \mathbf{T}^p, & \text{PTT,} \\ (\mathbf{T}^p)^2, & \text{Giesekus.} \end{cases} \quad (3)$$



# Natural stress formulation

Introducing the configuration tensor  $\mathbf{A}$  by

$$\mathbf{T}^P = \frac{1}{Wi} (\mathbf{A} - \mathbf{I}), \quad (4)$$

and expressing  $\mathbf{A}$  in terms of the dyadic products of  $\mathbf{v}$  and an orthogonal vector  $\mathbf{w}$  as follows:

$$\mathbf{A} = \lambda \mathbf{v} \mathbf{v}^T + \mu (\mathbf{v} \mathbf{w}^T + \mathbf{w} \mathbf{v}^T) + \nu \mathbf{w} \mathbf{w}^T, \quad (5)$$

where

$$\mathbf{v} = (u, v)^T, \quad \mathbf{w} = \frac{1}{|\mathbf{v}|} (-v, u)^T, \quad (6)$$

with  $\mathbf{w}$  chosen such that  $\|\mathbf{v} \times \mathbf{w}\| = 1$ .



# Natural stress formulation

Finally, the set of equation in this new formulation is given by

$$\begin{aligned} Wi [(\mathbf{v} \cdot \nabla) \lambda + 2\mu \nabla \cdot \mathbf{w}] + \left( \lambda - \frac{1}{|\mathbf{v}|^2} \right) + \kappa g_\lambda &= 0, \\ Wi [(\mathbf{v} \cdot \nabla) \mu + \nu \nabla \cdot \mathbf{w}] + \mu + \kappa g_\mu &= 0, \\ Wi [(\mathbf{v} \cdot \nabla) \nu] + (\nu - |\mathbf{v}|^2) + \kappa g_\nu &= 0, \end{aligned} \quad (7)$$

where

$$g_\lambda = \begin{cases} \left( \lambda |\mathbf{v}|^2 - 2 + \frac{\nu}{|\mathbf{v}|^2} \right) \left( \lambda - \frac{1}{|\mathbf{v}|^2} \right), & \text{PTT}, \\ \left( \lambda - \frac{1}{|\mathbf{v}|^2} \right)^2 |\mathbf{v}|^2 + \frac{\mu^2}{|\mathbf{v}|^2}, & \text{Giesekus}, \end{cases}, \quad g_\mu = \left( \lambda |\mathbf{v}|^2 - 2 + \frac{\nu}{|\mathbf{v}|^2} \right) \mu,$$
$$g_\nu = \begin{cases} \left( \lambda |\mathbf{v}|^2 - 2 + \frac{\nu}{|\mathbf{v}|^2} \right) (\nu - |\mathbf{v}|^2), & \text{PTT}, \\ (\nu - |\mathbf{v}|^2)^2 \frac{1}{|\mathbf{v}|^2} + \mu^2 |\mathbf{v}|^2, & \text{Giesekus}. \end{cases}$$
 (8)



# Stokesian solution

A discussion on the separable self-similar solutions for Stokes flow is given in the work of Richardson [11], noting the earlier work of Michael [12] and Moffatt [7]. Introducing the stream function  $\psi$ , the physically relevant dominant self-similar solution is

$$\psi \sim 2C_0 r^{\frac{3}{2}} \sin\left(\frac{\theta}{2}\right) \sin \theta, \quad p \sim 2\beta C_0 r^{-\frac{1}{2}} \sin\left(\frac{\theta}{2}\right), \quad \text{as } r \rightarrow 0. \quad (9)$$



## Behaviour along the streamlines (level curves)

The streamlines are level curves of the function  $\psi = C_0 r^{\frac{3}{2}} f(\theta)$  and parameterising each streamline by  $\theta$ , we have

$$r = \left( \frac{\psi}{C_0 f(\theta)} \right)^{\frac{2}{3}}. \quad (10)$$

Since  $dr/(rd\theta) = v_r/v_\theta$  holds along streamlines, then

$$\mathbf{v} \cdot \nabla = \frac{v_\theta}{r} \frac{d}{d\theta}, \quad (11)$$

where  $d/d\theta$  is the total derivative with respect to  $\theta$  along the streamline.



# System of ordinary differential equations

Since we consider the velocities as given, the constitutive equations is a system of ordinary differential equations (ODEs) along streamlines. In polar coordinates, the constitutive equations takes the form

$$\begin{aligned} \frac{v_\theta}{r} \frac{dT_{rr}^P}{d\theta} - 2 \frac{\partial v_r}{\partial r} T_{rr}^P - \frac{2}{r} \frac{\partial v_r}{\partial \theta} T_{r\theta}^P + \kappa g_{rr} + T_{rr}^P &= 2 \frac{\partial v_r}{\partial r}, \\ \frac{v_\theta}{r} \frac{dT_{r\theta}^P}{d\theta} + \frac{v_\theta}{r} T_{rr}^P - \frac{1}{r} \frac{\partial v_r}{\partial \theta} T_{\theta\theta}^P - \frac{\partial v_\theta}{\partial r} T_{rr}^P + \kappa g_{r\theta} + T_{r\theta}^P &= \left( \frac{1}{r} \frac{\partial v_r}{\partial \theta} - \frac{v_\theta}{r} + \frac{\partial v_\theta}{\partial r} \right), \\ \frac{v_\theta}{r} \frac{dT_{\theta\theta}^P}{d\theta} + 2 \frac{v_\theta}{r} T_{r\theta}^P - 2 \frac{\partial v_\theta}{\partial r} T_{r\theta}^P - \frac{2}{r} \frac{\partial v_\theta}{\partial \theta} T_{\theta\theta}^P - 2 \frac{v_r}{r} T_{\theta\theta}^P + \kappa g_{\theta\theta} + T_{\theta\theta}^P &= 2 \left( \frac{1}{r} \frac{\partial v_\theta}{\partial \theta} + \frac{v_r}{r} \right), \end{aligned} \quad (12)$$

$$\begin{aligned} g_{rr} &= \begin{cases} (T_{rr}^P + T_{\theta\theta}^P) T_{rr}^P, & \text{PTT,} \\ (T_{rr}^P)^2 + (T_{r\theta}^P)^2, & \text{Giesekus,} \end{cases} & g_{r\theta} &= T_{r\theta}^P (T_{rr}^P + T_{\theta\theta}^P), \\ g_{\theta\theta} &= \begin{cases} (T_{rr}^P + T_{\theta\theta}^P) T_{\theta\theta}^P, & \text{PTT,} \\ (T_{r\theta}^P)^2 + (T_{\theta\theta}^P)^2, & \text{Giesekus.} \end{cases} \end{aligned} \quad (13)$$



# Behaviour near the stick surface

For small values of  $\theta$ , at leading order in  $\theta$ , the stream function and velocity are

$$\psi \sim C_0 r^{\frac{3}{2}} \theta^2, \quad v_r \sim 2C_0 r^{\frac{1}{2}} \theta, \quad v_\theta \sim -\frac{3}{2} C_0 r^{\frac{1}{2}} \theta^2, \quad (14)$$

with the shear and radial strain rates

$$\dot{\gamma} \sim 2C_0 r^{-\frac{1}{2}}, \quad \dot{\epsilon} \sim C_0 r^{-\frac{1}{2}} \theta. \quad (15)$$



## Behavior near the stick surface

Since  $\theta \ll 1$ , the radial flow dominates the angular flow with also the shear rate dominating the radial strain rate. Using the constitutive equations and retaining only the leading-order terms in  $\theta$  gives

$$\begin{aligned} \frac{3}{2}\theta^2 \frac{dT_{rr}^p}{d\theta} + 2\theta T_{rr}^p + 4T_{r\theta}^p - \frac{r^{\frac{1}{2}}}{C_0} (\kappa g_{rr} + T_{rr}^p) &= -2\theta, \\ \frac{3}{2}\theta^2 \frac{dT_{r\theta}^p}{d\theta} + \frac{3}{4}\theta^2 T_{rr}^p + 2T_{\theta\theta}^p - \frac{r^{\frac{1}{2}}}{C_0} (\kappa g_{r\theta} + T_{r\theta}^p) &= -2, \\ \frac{3}{2}\theta^2 \frac{dT_{\theta\theta}^p}{d\theta} + \frac{3}{2}\theta^2 T_{r\theta}^p - 2\theta T_{\theta\theta}^p - \frac{r^{\frac{1}{2}}}{C_0} (\kappa g_{\theta\theta} + T_{\theta\theta}^p) &= 2\theta. \end{aligned} \quad (16)$$



## Behavior near the stick surface

For  $\theta \ll r^{\frac{1}{2}}$ , viscometric polymer stresses satisfy

$$\begin{aligned}\kappa g_{rr} + T_{rr}^P &= 2\dot{\gamma} T_{r\theta}^P, \\ \kappa g_{r\theta} + T_{r\theta}^P &= \dot{\gamma} (T_{\theta\theta}^P + 1), \\ \kappa g_{\theta\theta} + T_{\theta\theta}^P &= 0.\end{aligned}\tag{17}$$

For the Oldroyd-B model, Eq. (17) with  $\kappa = 0$  give the usual relationships

$$T_{\theta\theta}^P = 0, \quad T_{r\theta}^P = \dot{\gamma}, \quad T_{rr}^P = 2\dot{\gamma}^2.\tag{18}$$



## Behavior in the core region

On small radial distance  $r \ll 1$  near the singularity, but away from both surfaces, we have

$$1 \ll \mathbf{T}^P \ll \nabla \mathbf{v}, \quad \text{as } r \rightarrow 0. \quad (19)$$

Consequently the polymer constitutive equation reduces to

$$\overset{\nabla}{\mathbf{T}}^P = 0. \quad (20)$$

which has the exact so-called stretching solution

$$\mathbf{T}^P = \lambda(\psi) \mathbf{v} \mathbf{v}^T \quad \text{as } r \rightarrow 0, \quad (21)$$

where the function  $\lambda(\psi)$  is constant along streamlines.



# Core solution

Eq. (21) can be written, in Cartesian coordinates, as

$$\begin{aligned} T_{11}^P &= \lambda u^2, \\ T_{12}^P &= \lambda uv, \\ T_{22}^P &= \lambda v^2 \end{aligned} \tag{22}$$

The ansatz solution for  $\lambda$  is

$$\lambda = \frac{C_1}{C_0^2} \left( \frac{\psi}{C_0} \right)^{n_1}, \tag{23}$$

where  $n_1$  and  $C_1$  are constants to be determined.



## Core solution for small values of $\theta$

For small values of  $\theta$ , we can simplify the expressions for  $\psi$  (and the velocity components) and Eq. (22) as

$$\begin{aligned}\psi &\sim C_0 x^{-\frac{1}{2}} y^2, \\ u &\sim 2C_0 x^{-\frac{1}{2}} y, \quad v \sim \frac{1}{2} C_0 x^{-\frac{3}{2}} y^2, \\ T_{11}^p &\sim 4C_1 x^{-\frac{1}{2}n_1-1} y^{2n_1+2}, \quad T_{12}^p \sim C_1 x^{-\frac{1}{2}n_1-2} y^{2n_1+2}, \\ T_{22}^p &\sim \frac{1}{4} C_1 x^{-\frac{1}{2}n_1-3} y^{2n_1+4}.\end{aligned}\tag{24}$$



# Viscometric approximation breaks down

For small values of  $\theta$  the viscometric behaviour can be written as

$$\begin{aligned} T_{11}^p &\sim 8C_0^2x^{-1}, & T_{12}^p &\sim 2C_0x^{-\frac{1}{2}}, \\ T_{22}^p &\sim 0 \end{aligned} \tag{25}$$

Then, equating the viscometric (25) and core equations (24) we obtain the boundary layer thickness and the value of  $n_1$  given, respectively, by

$$\begin{aligned} y &= x^{\frac{3}{2}} \\ n_1 &= -\frac{6}{5} \end{aligned} \tag{26}$$



## Summary of the core behaviour

The singular polymer stress behavior is given by

$$\mathbf{T}^P \sim \begin{cases} r^{-\frac{4}{5}}, & \text{Oldroyd-B,} \\ r^{-\frac{4}{11}}, & \text{PTT,} \\ r^{-\frac{5}{16}}, & \text{Giesekus.} \end{cases} \quad (27)$$

We also can get the singular behavior for the natural stress variables for the three models

$$\lambda = \begin{cases} -\frac{9}{5}, & \text{Oldroyd-B,} \\ -\frac{15}{11}, & \text{PTT,} \\ -\frac{21}{16}, & \text{Giesekus,} \end{cases} \quad \mu = \begin{cases} -\frac{3}{10}, & \text{Oldroyd-B,} \\ -\frac{3}{22}, & \text{PTT,} \\ 0, & \text{Giesekus,} \end{cases}$$
$$\nu = \begin{cases} \frac{6}{5}, & \text{Oldroyd-B,} \\ \frac{12}{11}, & \text{PTT,} \\ \frac{21}{16}, & \text{Giesekus} \end{cases} \quad (28)$$



## Numerical results

We now present numerical results for the system of Eq. (16). For a numerical solution, we fix the streamline, i.e., the value of  $\psi$ , and solve the resulting system of ODEs. We start sufficiently far upstream, imposing viscometric stresses obtained from solving. The interval of integration for  $\theta$  is taken as  $[10^{-6}, \pi - 10^{-10}]$  and use Matlab's ode15s solver with  $\text{AbsTol} = \text{RelTol} = 10^{-6}$ . Parameter values in all simulations were  $\kappa = 0.1$  for



# Streamlines

To orient ourselves, Fig 4 shows selected streamlines that pass close to the singularity. Plotted are the stick and slip boundary layer curves.

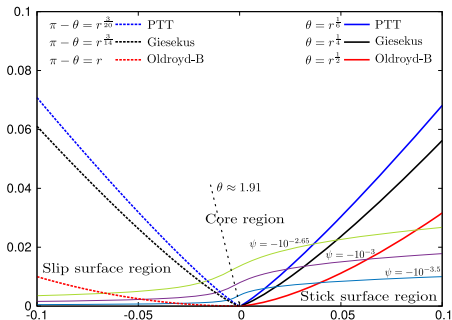


Figura 4: A plot of selected streamlines near the singularity, along with the boundary layer curves for all three models.



# Stress components along the streamline $\psi = -10^{-6}$ .

Figure 5 shows the polar stress components for all three models.

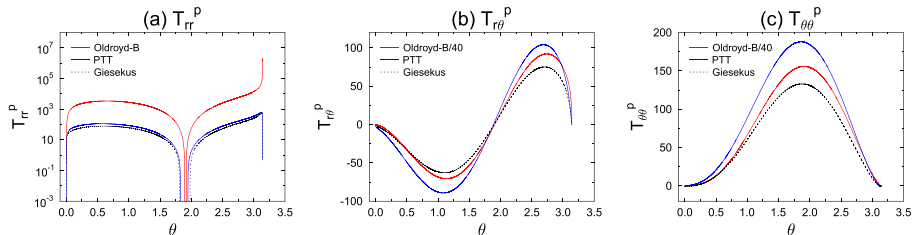


Figura 5: Stress components along the streamline  $\psi = -10^{-6}$ .



# Components of the dyadic tensor $\mathbf{v}\mathbf{v}^T$ along the streamline $\psi = -10^{-6}$ .

Figure 6 gives the components the dyadic tensor  $\mathbf{v}\mathbf{v}^T$  arising in the stretching solution.

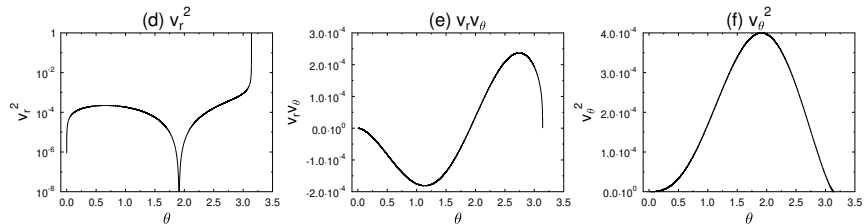


Figura 6: Components of the dyadic tensor  $\mathbf{v}\mathbf{v}^T$  along the streamline  $\psi = -10^{-6}$ .



# Estimates of $\lambda$ along the streamline $\psi = -10^{-6}$ .

This figure gives estimates of  $\lambda$  formed from the ratio of the appropriate components of stress and the dyadic product of the velocities.

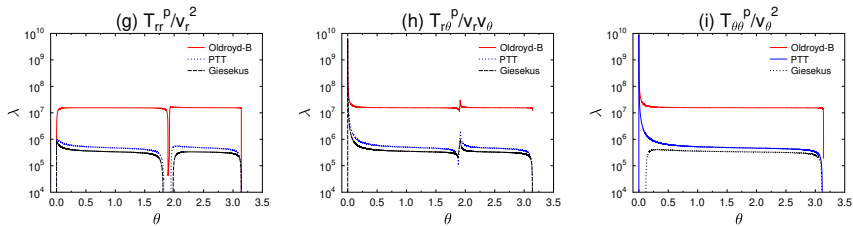


Figura 7: Estimates of  $\lambda$  along the streamline  $\psi = -10^{-6}$ .



# Slopes of the stress components: Oldroyd-B, PTT and Giesekus

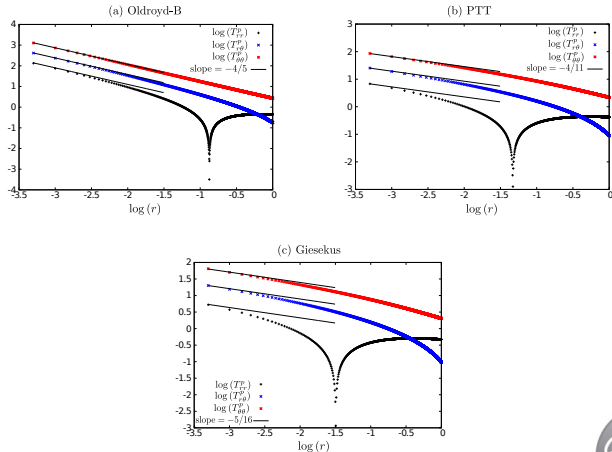


Figura 8: Slopes of the stress components along the line  $\theta = \frac{\pi}{2}$ .



# Slopes of the natural stress variables: Oldroyd-B, PTT and Giesekus

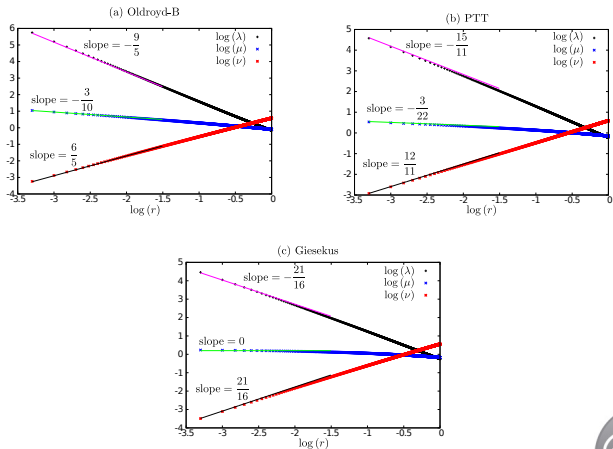


Figura 9: Slopes of the natural stress variables along the line  $\theta = \frac{\pi}{2}$ .



# Overview of the numerical method

We implement the numerical scheme in a finite-difference framework. The algorithm has two main steps:

- ① Computation of velocity and pressure fields: based on a semi-implicit scheme, velocity and pressure are uncoupled via an incremental projection method.
- ② Computation of the non-Newtonian tensor: After obtaining the final velocity and pressure fields, the final value for the polymer stress tensor  $(\mathbf{T}^p)^{n+1}$  is computed according to the two stress formulations.

For more details on the numerical method see the work of Evans et al. [3].



# Visualization details of the nonuniform mesh

Mesh	$\Delta x_{min}$	$\Delta y_{min}$
$M_1$	$5.0 \times 10^{-3}$	$5.0 \times 10^{-3}$
$M_2$	$5.0 \times 10^{-4}$	$5.0 \times 10^{-4}$
$M_3$	$5.0 \times 10^{-5}$	$5.0 \times 10^{-5}$

Tabela 1: Mehses used in the present work.

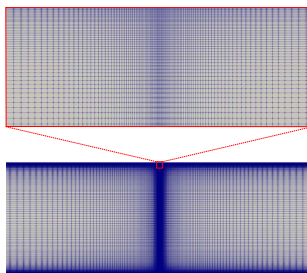


Figura 10: Visualization details of the nonuniform mesh



# Slopes using the full set of equations

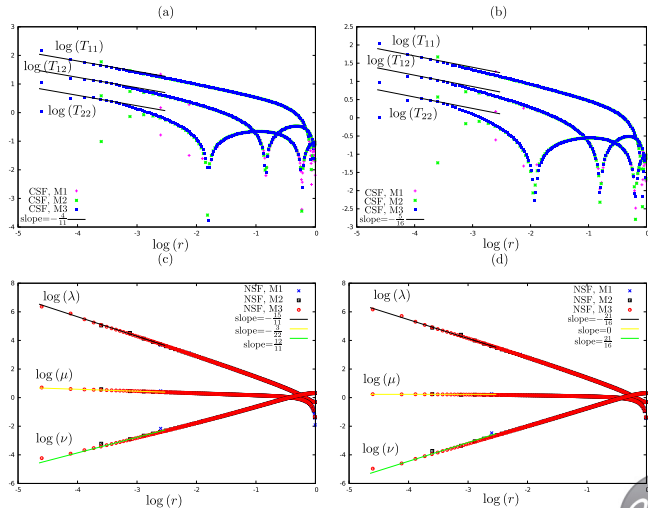


Figura 11: Asymptotic variation near the stick-slip transition point.



# Conclusion

- Stresses of PTT, Giesekus, and Oldroyd-B fluids near the stick-slip singularity were investigated.
- PTT, Giesekus, and Oldroyd-B models exhibited different behaviors in the proximity of the singularity.
- Understanding these stresses can help predict and control the behavior of viscoelastic fluids.
- The asymptotic results can aid numerical schemes, where an analytical solution in the neighbourhood of the singularity can be used to guide discretisations and improve accuracy.



- [1] J. D. Evans, I. L. Palhares Junior, C. M. Oishi. Stresses of PTT, Giesekus, and Oldroyd-B fluids in a Newtonian velocity field near the stick-slip singularity. *Physics of Fluids*, 29(12) (2017).
- [2] J. D. Evans, J. A. Cuminato, I. L. Palhares Junior, C. M. Oishi. Numerical study of the stress singularity in stick-slip flow of the Phan-Thien Tanner and Giesekus fluids. *Physics of Fluids*, 31(9) (2019).
- [3] J. D. Evans, H. L. França, C. M. Oishi, Application of the natural stress formulation for solving unsteady viscoelastic contraction flows, *Journal of Computational Physics*. 388 (2019) 462-489.
- [4] J. D. Evans, H. L. França, I. L. Palhares Junior, C. M. Oishi. Testing viscoelastic numerical schemes using the Oldroyd-B fluid in Newtonian kinematics. *Applied Mathematics and Computation*, (2020) 387, 125106.



- [5] M. Renardy, How to integrate the upper convected Maxwell (UCM) stresses near a singularity (and maybe elsewhere, too). *J. Non-Newtonian Fluid Mech.* 52(1) (1994) 91-95.
- [6] W.R. Dean, P.E. Montagnon, On the steady motion of viscous liquid in a corner, *Proc. Cambridge Philos. Soc.* 45 (1949) 389-394.
- [7] H.K. Moffatt, Viscous and resistive eddies near a sharp corner, *J. Non-Newtonian Fluid Mech.* 18 (1964) 1-18.
- [8] J. D. Evans. Re-entrant corner behaviour of the PTT fluid with a solvent viscosity. *J. Non-Newtonian Fluid Mech.*, 165 (2010) 527-537.
- [9] J. D. Evans. Re-entrant corner behaviour of the Giesekus fluid with a solvent viscosity. *J. Non-Newtonian Fluid Mech.*, 165 (2010) 538-543.
- [10] M. Renardy. The stresses of an upper convected Maxwell fluid in a Newtonian velocity field near a re-entrant corner. *J. Non-Newtonian Fluid Mech.*, 50 (1993) 127–134.



- [11] S. Richardson. A 'stick-slip' problem related to the motion of a free jet at low Reynolds numbers. In Mathematical Proceedings of the Cambridge Philosophical Society. 67 (1970) 477-489.
- [12] Michael, D. H. "The separation of a viscous liquid at a straight edge." Mathematika 5.1 (1958): 82-84.

